3 The Quantum Monte Carlo Method. Simple systems

In this section we shall demonstrate how the density matrix treatment of a system, S, coupled to a reservoir, may be replaced by a method in which wave functions are propagated according to the system Hamiltonian and certain random elements. The density matrix is then constructed as in Eq.(6) for an ensemble of such wave functions, which has to be sufficiently big to yield the expectation values of interest with sufficiently small statistical uncertainty. Such an approach has two main features of interest. First, if the relevant Hilbert space of the quantum system has a dimension N large compared to 1, the number of variables involved in a wave function treatment ($\sim N$) is much smaller than the one required for calculations with density matrices ($\sim N^2$). Second, new physical insight may be gained, in particular in the studies of the behaviour of a single quantum system.

The purpose of this section is to give a general presentation of the Quantum Monte Carlo method (QMC), and I shall present the method as it has been formulated in Refs.[3, 4, 5]. The idea of writing the master equation in terms of a stochastic process for wave functions has been put forward by a number of groups within the last few years. A, maybe, surprising variation in the motivation, methods and goals between these groups exists, and I shall discuss some applications of the theory, also by other groups.

3.1 Simulations for laser excited two-level atoms

3.1.1 How to do it

We present first the method in the simple case of a two-level atom, states $|g\rangle$, $|e\rangle$, coupled to the quantized electromagnetic field [3].

When solving Schrödinger's equation for the atomic wavefunction we include in the equation for the excited state amplitude, c_e, a decay term, $(\dot{c}_e)_{decay} = -\frac{\Gamma}{2}c_e$. This correction term corresponds to adding the imaginary part $-i\hbar\Gamma/2$ to the energy of the unstable excited state, as it is sometimes done in scattering theory to incorporate decay effects:

$$H_S \rightarrow H \equiv H_S - \frac{i\hbar\Gamma}{2}|e\rangle\langle e|. \qquad (47)$$

We now propagate the wavefunction amplitudes in time, and at each time step, δt, we make a choice: either the wavefunction is normalized which is necessary because the decay term in (47) both reduces the excited state amplitude *and the total norm* of the wave function, or the system performs a quantum jump, and the wave function is put equal to the ground state wave function, $|g\rangle$. The jump occurs with probability $\delta p = \Gamma|c_e|^2\delta t$, which is compared with a number ϵ chosen at random within the interval

[0, 1]: if $\epsilon < \delta p$ the jump occurs. This evolution is then repeated over and over again with a new random number ϵ at each time increment.

In part (a) of Fig.3 is shown the result of such an evolution. The parameters are a vanishing detuning δ between the laser and atomic frequencies, and a Rabi frequency $\Omega = 3\Gamma$. We have plotted the excited state population $|c_e|^2$ as a function of time for a single wave function, and we see the characteristic Rabi-oscillations of this population. At different points in time, jumps occur, two are shown in the figure with vertical dashed lines, and the evolution proceeds. Part (b) of the figure shows the average population of the excited state for 100 wave functions, and a dotted line indicates the solution to the master equation for $\rho_{ee}(t)$. It works ! (A formal proof of this is presented in Section 3.2.2.)
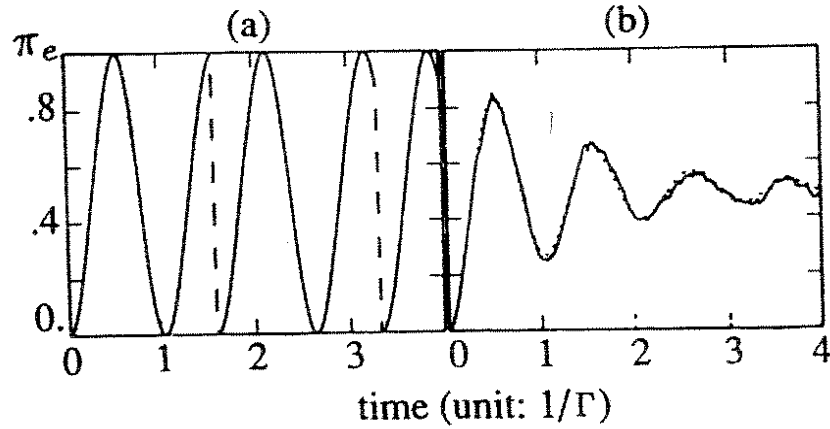

Figure 3: (a) Time evolution of the excited-state population of a two-level atom in the QMC approach. The dashed lines indicate the projection of the atomic wave function onto the ground state (quantum jump). (b) Excited state population averaged over 100 wave functions all starting in the ground state at time 0. The dotted line represents the master equation result.

3.1.2 A physical interpretation of the procedure

We now discuss the physical content of the QMC procedure. We consider at time $t = 0$ a two-level atom in a superposition of the ground and excited states

$$|\phi(0)\rangle = c_g|g\rangle + c_e|e\rangle, \tag{48}$$

and we omit the laser field and put $\delta = 0$ so that H_S vanishes in the rotating wave approximation.

In the QMC formalism, following the first step of the evolution just outlined, we have at time δt :

$$|\phi^{(1)}(\delta t)\rangle = c_g|g\rangle + c_e e^{-\Gamma\delta t/2}|e\rangle. \tag{49}$$

The probability δp for making a quantum jump is:

$$\delta p = \Gamma |c_e|^2 \delta t \qquad (50)$$

and this corresponds to the probability for emitting a photon between 0 and δt. Indeed, the wave function $|\phi^{(1)}(\delta t)\rangle$ in (49) is nothing but the zero-photon component of the total atom+field wave function in (12), and the difference, $1 - \langle \phi^{(1)} | \phi^{(1)} \rangle \simeq \Gamma |c_e|^2 \delta t$ is the total norm of the remaining one-photon component, having the atom in its ground state. Thus, our random choice simulates the result of the measurement of the number of photons emitted between 0 and δt, and the quantum jump is the projection of the wave function onto the ground state $|g\rangle$, associated with the detection of one photon. In the absence of laser light the wave function has no further evolution.

If no quantum jump occurs, the normalized wave function $|\phi(\delta t)\rangle$ is proportional to $|\phi^{(1)}(\delta t)\rangle$. Using the fact that δt is small, we get after normalization:

$$|\phi(\delta t)\rangle = c_g \left(1 + \frac{\Gamma \delta t}{2} |c_e|^2 \right) |g\rangle + c_e \left(1 - \frac{\Gamma \delta t}{2} |c_g|^2 \right) |e\rangle. \qquad (51)$$

We note that there has been a slight rotation of the wave function: the probability amplitude for being in the ground state has increased, and the one for being in the excited state has decreased. The non-hermitian part of the evolution corresponds to the modification of the state of the system associated with a zero detection result of the number of emitted photons. The information gained in *a zero result experiment* and its consequences for the evolution of the system has been emphasised by Dicke [30].

The rotation following a zero detection result is essential. If it did not occur, i.e., if we were to take the wave function

$$|\phi(\delta t)\rangle = |\phi(0)\rangle, \qquad (52)$$

the probability for having a quantum jump (i.e. detecting a photon) between δt and $2\delta t$ would be equal to the one between 0 and δt, and this would repeat over and over until a quantum jump would finally occur. Even for very small values $|c_e|^2 \neq 0$, one would then always find that a photon is emitted between $t = 0$ and $t = \infty$, and this would clearly be wrong. Due to the slight rotation in (51) however, the probability for making a quantum jump between δt and $2\delta t$ is smaller, and it will be further reduced as no quantum jump occurs in successive time steps. Assuming that no quantum jump occurred between 0 and t, we can write $|\phi(t)\rangle$ as:

$$|\phi(t)\rangle = \frac{c_g |g\rangle + c_e e^{-\Gamma t/2} |e\rangle}{\sqrt{|c_g|^2 + |c_e|^2 e^{-\Gamma t}}}. \qquad (53)$$

The probability $P(t)$ for having no quantum jump between 0 and t fulfils the equation

$$P(t + \delta t) = P(t)[1 - \Gamma \delta t |c_e|^2 e^{-\Gamma t} / (|c_g|^2 + |c_e|^2 e^{-\Gamma t})] \qquad (54)$$

and this equation has the solution

$$P(t) = |c_g|^2 + |c_e|^2 e^{-\Gamma t}. \qquad (55)$$

This shows, as we would have expected, that there is a probability $|c_g|^2$ that no jump occurs between $t = 0$ and $t = \infty$.

Our procedure explicitly solves the riddle: How can n atoms, all being initially in a coherent superposition (48), relax towards the ground state without giving us n fluorescence photons resulting in a macroscopic violation of energy conservation ? Answer: only a fraction $|c_e|^2$ of the atoms decay by photon emission, the remaining fraction of atoms correspond to the wave function component $c_g|g\rangle \otimes |0\rangle$ in (12), i.e. to atoms being in the ground state already. Our simulation provides a way for these atoms to "get rid of" their excited state components without emission of light.

We also note that at any time the ensemble consists of only two kinds of wave functions: the ground state $|g\rangle$ and the state $|\phi(t)\rangle$ (53). It is easy to show that the mean values of products $\overline{c_i c_j^*}$, $i, j = e, g$, obey the equations (13). The two wave functions have no particular relations with the state vectors that diagonalize ρ. The uniqueness (up to degeneracies) of the eigenstate basis is also shown to be less important: our wave functions are not even orthogonal.

Note that the measurement is performed on the reservoir and *not* on the system variables. One may invoke the argument [10] that since photons emitted by the atom play no further role in its future evolution, they may as well be detected and absorbed, and this detection leads, by the rules of quantum measurements, to the wavefunction evolution described. Considering the ensuing evolution of ensemble averages, we have then obtained an alternative derivation of the master equation.

3.2   General presentation of the QMC procedure

3.2.1   How to do it in the general case

We now present the procedure for evolving wave functions of a general small system so that the ensemble average in the sense of Eq.(6) can replace the solution to the master equation (11):

$$\frac{d}{dt}\rho = \frac{1}{i\hbar}[H_S, \rho] + \mathcal{L}_{\text{relax}}[\rho], \qquad (56)$$

with $\mathcal{L}_{\text{relax}}[\rho]$ being of the general Lindblad form (18),

$$\mathcal{L}_{\text{relax}}[\rho] = -\frac{1}{2}\sum_i (C_i^+ C_i \rho + \rho C_i^+ C_i) + \sum_i C_i \rho C_i^+. \qquad (57)$$

Consider the normalized wave function $|\phi(t)\rangle$. In order to get the wave function at time $t + \delta t$, we proceed in two steps:
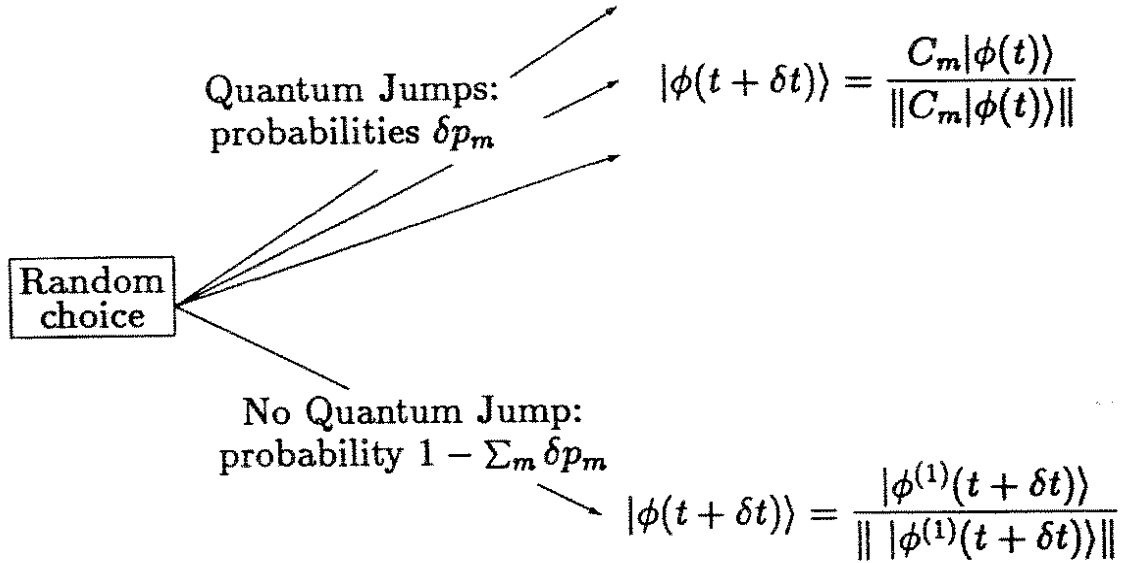
$$\text{Quantum Jumps:} \quad |\phi(t+\delta t)\rangle = \frac{C_m |\phi(t)\rangle}{\| C_m |\phi(t)\rangle \|}$$

Quantum Jumps: probabilities δp_m

Random choice

No Quantum Jump: probability $1 - \Sigma_m \, \delta p_m$

$$|\phi(t+\delta t)\rangle = \frac{|\phi^{(1)}(t+\delta t)\rangle}{\| \, |\phi^{(1)}(t+\delta t)\rangle \|}$$

Figure 4: *The possible quantum jumps in the Monte-Carlo evolution*

1. First we calculate the wave function $|\phi^{(1)}(t+\delta t)\rangle$ obtained by evolving $|\phi(t)\rangle$ with the non hermitian Hamiltonian:

$$H = H_S - \frac{i\hbar}{2} \sum_m C_m^\dagger C_m. \tag{58}$$

This gives for sufficiently small δt:

$$|\phi^{(1)}(t+\delta t)\rangle = \left(1 - \frac{iH\delta t}{\hbar} \right) |\phi(t)\rangle. \tag{59}$$

Since H is not hermitian, this new wave function is not normalized. The square of its norm is:

$$
\begin{aligned}
\langle \phi^{(1)}(t+\delta t) | \phi^{(1)}(t+\delta t) \rangle &= \langle \phi(t) | \left(1 + \frac{iH^\dagger \delta t}{\hbar} \right) \left(1 - \frac{iH\delta t}{\hbar} \right) |\phi(t)\rangle \\
&= 1 - \delta p,
\end{aligned} \tag{60}
$$

where δp reads:

$$\delta p = \delta t \, \frac{i}{\hbar} \, \langle \phi(t) | H - H^\dagger | \phi(t) \rangle = \sum_m \delta p_m \tag{61}$$

$$\delta p_m = \delta t \, \langle \phi(t) | C_m^\dagger C_m | \phi(t) \rangle \geq 0. \tag{62}$$

The magnitude of the step δt is adjusted so that this calculation to first order is valid; in particular it requires $\delta p \ll 1$.

27

2. The second step of the evolution of $|\phi\rangle$ between t and $t + \delta t$ is connected with the possibility of a quantum jump. In order to decide whether the jump occurs or not, we choose a random number ϵ, uniformly distributed between 0 and 1, and we compare it with δp. If δp is smaller than ϵ, which is most often the case since $\delta p \ll 1$, no quantum jump occurs, and we take for the new normalized wave function at $t + \delta t$:

$$\delta p < \epsilon : \quad |\phi(t + \delta t)\rangle = \frac{|\phi^{(1)}(t + \delta t)\rangle}{\sqrt{1 - \delta p}}. \tag{63}$$

If $\epsilon < \delta p$, a quantum jump takes place and we choose the new normalized wave function among the different states $C_m|\phi(t)\rangle$, according to the probability law $\Pi_m = \delta p_m / \delta p$:

$$\delta p > \epsilon : \quad |\phi(t + \delta t)\rangle = \frac{C_m|\phi(t)\rangle}{\sqrt{\delta p_m / \delta t}} \quad \text{with a probability } \Pi_m = \frac{\delta p_m}{\delta p}. \tag{64}$$

For the particular case of a two-level atom coupled to the vacuum electromagnetic field, these two steps coincide with the ones given above. In Ref.[4] a number of examples with various possibilities for H_S and the C_i-operators are given.

We can also extend the treatment of the no quantum jump periods to the general case. Suppose that we know that no quantum jump has occured between 0 and t. During this period the wave function obeys a non linear differential equation deduced from (58), (59) and (63):

$$i\hbar \frac{d|\phi\rangle}{dt} = \left(H + \langle\phi|\frac{H^\dagger - H}{2}|\phi\rangle \right) |\phi\rangle. \tag{65}$$

The solution of this equation is, for a time independent Hamiltonian:

$$|\phi(t)\rangle = \frac{e^{-iHt/\hbar}|\phi(0)\rangle}{\sqrt{\langle\phi(0)|e^{iH^\dagger t/\hbar}e^{-iHt/\hbar}|\phi(0)\rangle}} \tag{66}$$

which generalises (53). This corresponds to an evolution with the non-hermitian Hamiltonian between 0 and t:

$$i\hbar \frac{d|\phi\rangle}{dt} = H|\phi\rangle \tag{67}$$

and a subsequent normalization.

The no-jump evolution and the associated probability, e.g. $P(t)$ in Eq. (55), have been considered previously in an analysis of the quantum jump phenomenon in three level atoms. Dalibard and Cohen-Tannoudji [2] pointed out that $P(t)$ is a delay function providing the statistics of the time intervals between subsequent emission events. Identifying two very different time scales, they were able to derive the existence of dark and bright periods in the fluorescence signal as it had been observed experimentally. Zoller *et.al.* [31] gave a nice demonstration of this by numerical simulations.

If the no-jump conditioned wave function and the delay function are known analytically, they may constitute a very efficient simulation scheme: instead of making a decision at each time step, one applies the no-jump evolution (66) until the delay function reaches a certain value ϵ. Then a jump is made, following (64), and a new random value of ϵ is chosen, and one repeats the procedure. In fact, this procedure also applies in the case where $P(t)$ and the wave function have to be determined numerically, and it may represent a means to avoid exhausting the random number generator, and to weaken the demands on its uniformity and absence of correlations at very small values (remember that the jump in (64) occurs only if $\epsilon < \delta p \ll 1$).

3.2.2 Proof of equivalence with the Master Equation

With the set of rules in Eqs.(58) through (64), we can propagate a wave function $|\phi(t)\rangle$ in time, and we now show that this procedure is equivalent to the master equation (56). More precisely we consider the quantity $\bar{\sigma}(t)$ obtained by averaging $\sigma(t) = |\phi(t)\rangle\langle\phi(t)|$ over the various outcomes at time t of the QMC evolutions, all starting in $|\phi(0)\rangle$, and we prove that $\bar{\sigma}(t)$ coincides with $\rho(t)$ at all times t, provided they coincide at $t = 0$.

Consider a QMC wave function $|\phi(t)\rangle$ at time t. At time $t + \delta t$, the average value of $\sigma(t + \delta t)$ over the evolution caused by different values of the random number ϵ is:

$$\overline{\sigma(t + \delta t)} = \quad (1 - \delta p) \frac{|\phi^{(1)}(t + \delta t)\rangle}{\sqrt{1 - \delta p}} \frac{\langle\phi^{(1)}(t + \delta t)|}{\sqrt{1 - \delta p}}$$
$$+ \quad \delta p \sum_m \Pi_m \frac{C_m|\phi(t)\rangle}{\sqrt{\delta p_m/\delta t}} \frac{\langle\phi(t)|C_m^\dagger}{\sqrt{\delta p_m/\delta t}} \tag{68}$$

which gives

$$\overline{\sigma(t + \delta t)} = \sigma(t) + \frac{i\delta t}{\hbar}[\sigma(t), H_S] + \delta t \, \mathcal{L}_{\text{relax}}[\sigma(t)]. \tag{69}$$

When averaged over the possible values of $\sigma(t)$ this equation is equivalent to the master equation (56). If we assume that $\rho(0) = |\phi(0)\rangle\langle\phi(0)|$, $\bar{\sigma}(t)$ and $\rho(t)$ coincide at any time. In the case where $\rho(0)$ does not correspond to a pure state, one may first decompose it as a statistical mixture of pure states, $\rho(0) = \sum p_i|\chi_i\rangle\langle\chi_i|$ and choose the initial wave functions among the $|\chi_i\rangle$ with the weight factors p_i.

3.3 Getting good statistics with the QMC method

The master equation approach and the reduced density matrix give access to expectation values $\langle A\rangle(t) = \text{Tr}(\rho(t)A)$. This is also the primary goal of the QMC method. Applying the QMC method with n wave functions, we obtain the sample mean:

$$\langle A\rangle_{(n)}(t) = \frac{1}{n}\sum_{i=1}^n \langle\phi^{(i)}(t)|A|\phi^{(i)}(t)\rangle. \tag{70}$$

This value approximates $\langle A \rangle(t)$ with a statistical error $\delta A_{(n)}$ related to the square root of the sample variance $(\Delta A)^2_{(n)}$ by:

$$\delta A_{(n)} = \frac{\Delta A_{(n)}}{\sqrt{n}} \tag{71}$$

with:

$$(\Delta A)^2_{(n)}(t) = \frac{1}{n} \left(\sum_{i=1}^{n} \langle \phi^{(i)}(t) | A | \phi^{(i)}(t) \rangle^2 \right) - \langle A \rangle^2_{(n)}(t). \tag{72}$$

This is illustrated in Fig.3(b), with $A = |e\rangle\langle e|$. The QMC result is in good agreement with the one derived from the master equation (Optical Bloch Equations). Error bars inferred from (71) are not shown, but they may be estimated from the fluctuations of the curve in the figure.

The condition for a good signal to noise ratio $\langle A \rangle / \delta A_{(n)}$ can be written

$$\sqrt{n} \gg \frac{\Delta A_{(n)}(t)}{\langle A \rangle(t)} \tag{73}$$

In order to discuss the requirements imposed by (73), we now distuingish between two kinds of operators. First there are "local operators", such as the ones giving the population of a particular state $|j\rangle$, $A = |j\rangle\langle j|$ and $A^2 = A$. For those operators we expect :

$$\langle A \rangle(t) \sim \frac{1}{N}, \quad (\Delta A)^2(t) \sim \frac{1}{N}, \quad N \gg 1, \tag{74}$$

where N denotes the total number of quantum states involved in the simulation. If we insert these values in (73), we see that the number of simulations n must be larger than the number of states N. The Monte-Carlo treatment is not efficient in this case since the amount of calculation for determining a single $|\phi(t)\rangle$ is reduced by a factor of N with respect to the calculation of the density matrix $\rho(t)$, but one has to perform n QMC runs to get good statistics, with $n \geq N$.

The QMC treatment is more efficient if one deals with "global operators", such as the population of a large group of states, or, for the description of laser cooling, the average kinetic energy. For those operators, we have:

$$\Delta A(t) \sim \langle A \rangle(t). \tag{75}$$

In this case we see from (73) that good statistics is obtained after n Monte-Carlo runs as soon as n is much larger than unity. If one requires, say, a 10% accuracy for the average of global operators, the inequality (73) suggests $n \simeq 100$. Thus, when the number N of states involved is larger than this number, the QMC treatment should be more efficient than the master equation approach.

3.4 Doppler cooling

We now consider the example of 1-D Doppler cooling of a two-level atom, for which we present some numerical results. This will illustrate the efficiency of the QMC method as compared with the master equation approach when the number of states is not very low.

An atom with a transition between levels with angular momenta J_g and $J_e = J_g + 1$ is placed in a σ_+ polarized standing wave. Owing to optical pumping only the Zeeman sublevels $|g, m_g = J_g\rangle$ and $|e, m_e = J_e\rangle$ play a role and for simplicity we denote these substates $|g\rangle$ and $|e\rangle$ in the following. Doppler cooling occurs for negative values of the detuning $\delta = \omega_L - \omega_A$ between the laser and atomic frequencies; it originates from the fact that a moving atom is closer to resonance with the counterpropagating component of the wave than with the copropagating one; the atom therefore experiences a net radiation pressure force opposed to its velocity [32, 33]. This picture works well at non saturating laser intensities, where one may add the effects of the two waves independently. At higher intensities this type of semi-classical analysis based on the calculation of a damping force becomes more complicated [34, 35] and a quantum treatment of the atomic external motion is a good alternative. We present here the result of such an analysis using both the master equation and the QMC approach.

Within the rotating wave approximation the hamiltonian H_S reads

$$H_S = \frac{P^2}{2M} - \hbar\Omega \cos(kZ)(|e\rangle\langle g| + |g\rangle\langle e|) - \hbar\delta|e\rangle\langle e|, \tag{76}$$

where Z and P are the atomic position and momentum operators and Ω is the Rabi frequency of each travelling wave forming the standing wave. We choose the initial wave function $|\phi(0)\rangle$ equal to a momentum eigenstate $|g, p = 0\rangle$. At any later time t, $|\phi(t)\rangle$ is of the form:

$$|\phi(t)\rangle = \sum_n \alpha_n(t)|g, p = p_0 + 2n\hbar k\rangle + \beta_n(t)|e, p = p_0 + (2n+1)\hbar k\rangle \tag{77}$$

where the momentum p_0 depends on the random recoils associated with the spontaneous emission events which have occurred between 0 and t. The evolution of α_n and β_n consists of sequences of two steps. First the wave function evolves linearly with the non-hermitian Hamiltonian $H = H_S - i\hbar\frac{\Gamma}{2}|e\rangle\langle e|$:

$$i\dot{\alpha}_n = \frac{(p_0 + 2n\hbar k)^2}{2M\hbar}\alpha_n - \frac{\Omega}{2}(\beta_n + \beta_{n-1}) \tag{78}$$

$$i\dot{\beta}_n = \left(\frac{(p_0 + (2n+1)\hbar k)^2}{2M\hbar} - \delta - \frac{i\Gamma}{2}\right)\beta_n - \frac{\Omega}{2}(\alpha_n + \alpha_{n+1}). \tag{79}$$

Then we decide whether a quantum jump occurs. The probability δp for a jump is proportional to the total excited state population:

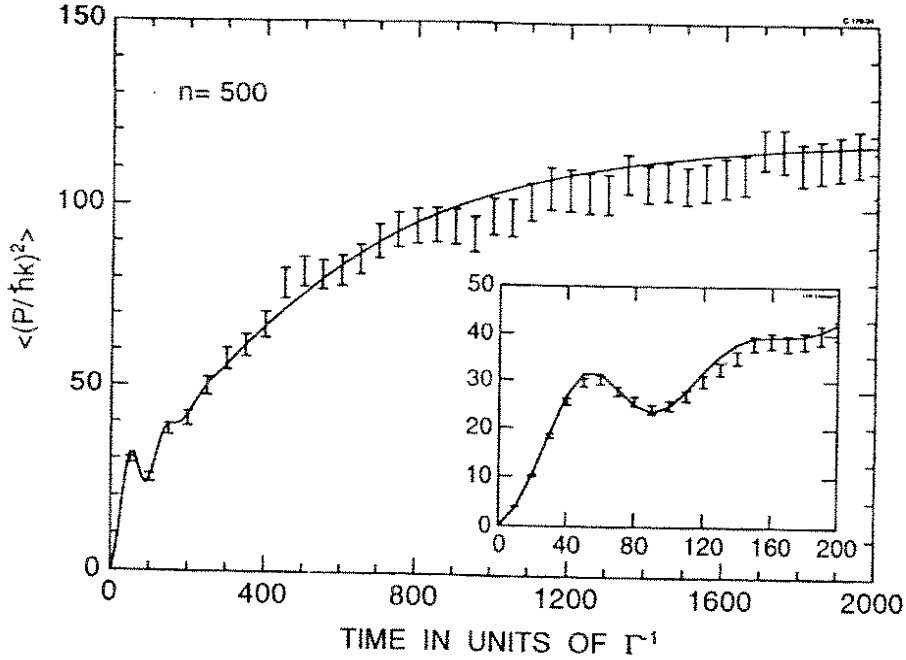$$\delta p = \Gamma \sum_n |\beta_n|^2 \delta t. \tag{80}$$

Figure 5: *Time evolution of $\langle P^2 \rangle$ in Doppler cooling. Time is measured in units of the excited state lifetime Γ^{-1} and momentum in units of $\hbar k$. The detuning δ and the Rabi frequency Ω are given by $\Omega = -\delta = \Gamma/2$. The atomic mass is such that $\Gamma = 200 \hbar k^2/M$. The points represent the Monte-Carlo results, obtained by averaging over $n = 500$ evolutions. The error bars correspond to the statistical error $\delta P^2_{(n)}$. We have also indicated, by a solid curve, the results of the density matrix approach. Both calculations involve 200 quantum states, and require approximately the same computing time on a scalar machine. We have detailed in the insert the short-time regime corresponding to the diffraction of the atomic de Broglie wave by the laser standing wave.*

If no quantum jump occurs, we simply normalize the wave function. If a jump occurs, the momentum $\hbar k'$ along the z axis of the fluorescence photon is chosen according to the probability distribution $\mathcal{N}(k') = \frac{3}{8}(1 + (\frac{k'}{k})^2)$ [39], and the new wave function is obtained by the action of one of the operators:

$$C_{k'} = \sqrt{\Gamma \mathcal{N}(k')}e^{-ik'Z}|g\rangle\langle e| \tag{81}$$

on $|\phi(t)\rangle$ [7]. This leads to:

$$
\begin{aligned}
\alpha_n(t + \delta t) &= \mu \beta_n(t) \\
\beta_n(t + \delta t) &= 0 \\
p_0 &\rightarrow p_0 - \hbar k'
\end{aligned}
\tag{82}
$$

where μ is a normalization coefficient. We note that in this way the recoil due to spontaneous emission is treated in an exact manner. In the master equation approach, an exact treatment of the spontaneous recoil requires a discretisation of atomic momenta on a grid with a step size small compared to $\hbar k$. This increases the amount of

---

[7]In the master equation the sum over i in Eq.(57) is replaced by an integral over the continuous variable k'.
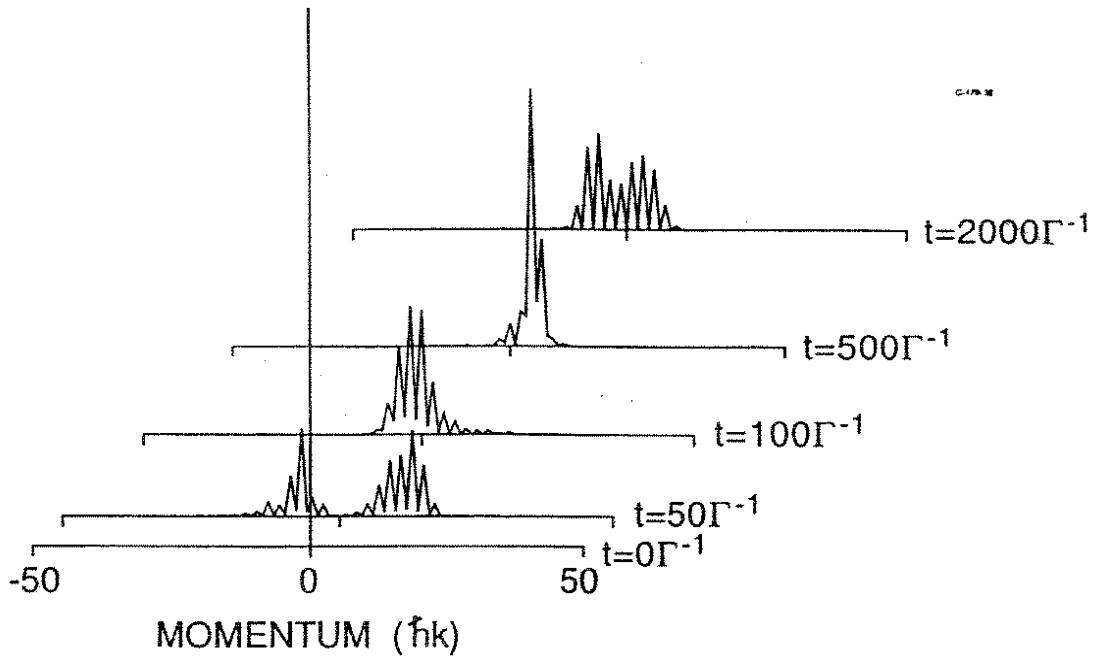
Figure 6: *Time evolution of the momentum distribution for a single Monte-Carlo wave function for the Doppler cooling situation described in Fig. 5. The MCWF extends over approximately $5\hbar k$ and explores as time goes on all significant parts of the momentum space.*

calculation with the master equation with respect to the QMC one, in addition to the N^2 versus N difference.

We have considered the case of sodium atoms ($\Gamma = 200\ \hbar k^2/M$), for which the minimum Doppler cooling limit, obtained for $\delta = -\Gamma/2$ and $\Omega \ll \Gamma$, corresponds to $p_{r.m.s.} \simeq 8.4\hbar k$. We have discretized the momentum in units of $\hbar k$ between $-50\ \hbar k$ and $+50\ \hbar k$ which corresponds to a basis with 202 eigenstates, with at any time 101 nonzero coefficients α_n and β_n (see (78,79)). p_0 is either an odd or even multiple of $\hbar k$ (with our discretization, chosen to make a comparison with the master equation, we take k' in (82) to be either 0 or $\pm k$ with probabilities $3/5, 1/5, 1/5$).

The results for the evolution of the sample mean $\langle P^2 \rangle_{(n)}$, defined as:

$$\langle P^2 \rangle_{(n)}(t) = \frac{1}{n} \sum_{i=1}^{n} \langle \phi^{(i)}(t)|P^2|\phi^{(i)}(t)\rangle, \tag{83}$$

are given in Fig. 5 together with the results for $\langle P^2 \rangle(t)$ obtained using the master equation treatment. These results correspond to the parameters $\Omega = -\delta = \Gamma/2$. The QMC results have been obtained as the average of $n = 500$ evolutions.

We clearly see in Fig. 5 the existence of two regimes in the evolution of $\langle P^2 \rangle(t)$. At short times, the number of spontaneous events is small, and the physics involved is essentially the diffraction of the plane atomic de Broglie wave by the grating formed by the laser standing wave [36]. For longer interaction times, dissipation comes into play [37, 38] and $\langle P^2 \rangle(t)$ tends to a steady-state value, of the order of $(11\hbar k)^2$. This

value for $p_{\text{r.m.s.}}$ is larger than the Doppler cooling limit (8.4 $\hbar k$) because of saturation effects.

We have indicated in Fig. 5 the statistical error $\delta P^2_{(n)}$ on the determination of $\langle P^2 \rangle_{(n)}$. This quantity $\delta P^2_{(n)}$, which was defined in (71,72), gives an estimate of the quality of the result, and with $n = 500$ wave functions, the *signal-to-noise* ratio in the range of 20 is quite satisfactory. On a computer we found that the time required for the calculation with 500 wave functions is equal to the time required for the master equation evolution. Therefore, even for this relatively simple 1D problem with "only" 200 states, the QMC method is at least as efficient as the master equation approach for determining cooling limits with a good precision .

Fig. 6 shows the evolution of the momentum distribution of a single wave function. The state extends over approximately $5\hbar k$ and explores, as time goes on, all the significant parts of the momentum space.

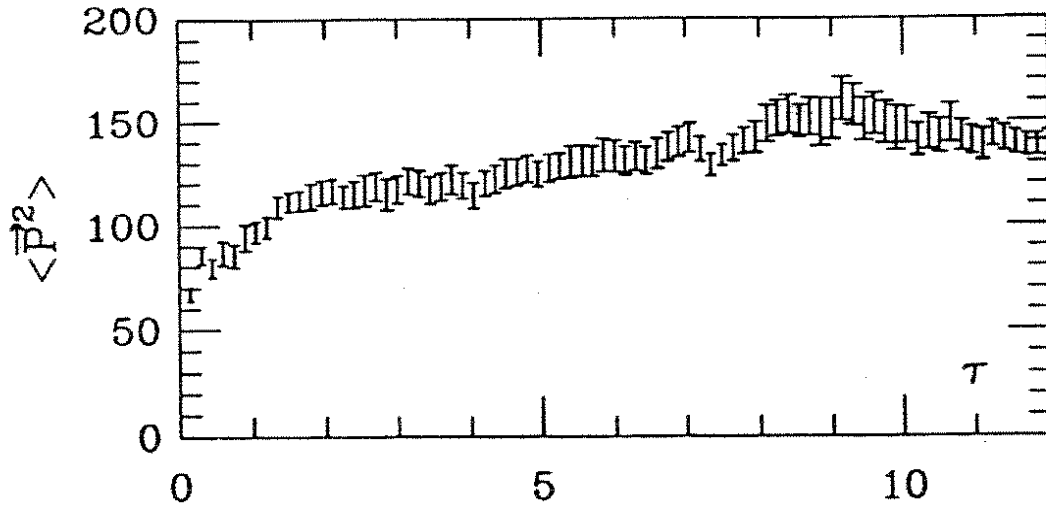## 3.5   Other numerical applications

Figure 7: *Temporal evolution of $\langle \vec{P}^2 \rangle$ in a 3D laser configuration formed by three mutually orthogonal standing waves of circular polarization. Time is given in the reduced unit, $\tau = \hbar k^2 t / M$. The results have been obtained as an average over 29 Monte Carlo wave functions, and the steady state results, $p_{\text{r.m.s}} \simeq 7.0 \pm 0.3\hbar k$ along each axis, are in good agreement with typical experimental values.*

One of our motivations for developing the QMC method was to be able to deal with laser cooling problems where the number of variables is very big. We have now developed a general program which allows calculations on cooling of atoms with arbitrary angular momentum values J_g, J_e in three dimensional laser field configurations. For practical reasons we are limited to a finite grid in momentum space, as in the application to Doppler cooling, and so far the maximum degeneracies considered correspond to $J_g = 4$, $J_e = 5$, the values for a much studied transition in the Cs atom. In Fig.7 we show results similar to the ones in Fig.5, but for 3D cooling of atoms with $J_g = 1$, $J_e = 2$

[40]. These calculations, performed with 29 wave functions only, give already quite a good prediction for the temperatures. They also show one of the problems in dealing with statistically scattered data: when has a stationary state been attained, which variations in the results are physical and which ones are statistical fluctuations ? In this case we have wave functions with $\simeq 10^5$ amplitudes, and there is no possibility to compare with density matrix results as in Fig.5.

Dum *et al* [9] have applied simulations to the laser cooling of trapped ions in a regime where comparisons with density matrix results are possible. Carmichael *et al* [6, 41] have considered a number of cavity field problems, and groups in Oxford [42] and in Helsinki [43] have made calculations for ultra-slow atomic collisions in laser fields.